Geochemical Perspectives Letters

Enhanced continental weathering activity at the onset of the mid-Cenomanian Event (MCE)

L. Nana Yobo, A.D. Brandon, L.M. Laukner, J.S. Eldrett, S.C. Bergman, D. Minisini

Supplementary Information

The Supplementary Information includes:

- Stratigraphic Framework
- Materials and Analytical Method
- Table S-1
- Figure S-1
- Supplementary Information References

Stratigraphic Framework

The middle Cenomanian Event (MCE) has been identified in stable carbon isotope ($\delta^{13}C$) records from marine carbonate and organic carbon records (*e.g.*, Paul *et al.*, 1994; Mitchell, 1996; Mitchell *et al.*, 1996; Mitchell and Carr, 1998; Stoll and Schrag, 2000; Jarvis *et al.*, 2001, 2006; Coccioni and Galeotti, 2003; Li *et al.*, 2006; Wilmsen, 2007; Gale *et al.*, 2002, 2008; Friedrich *et al.*, 2009; Gertsch *et al.*, 2010; Joo and Sageman, 2014; Andrieu *et al.*, 2015; Eldrett *et al.*, 2015; Gambacorta *et al.*, 2015) with a characteristic dual positive $\delta^{13}C$ excursion consisting of two $\delta^{13}C$ maxima (MCE a and MCE b; Mitchell *et al.*, 1996) and thus is considered a global event.

In Iona-1, the MCE interval is also characterised by a dual positive $\delta^{13}C$ excursion. The $\delta^{13}C$ data presented here is based on bulk organic matter after Eldrett *et al.* (2015) and the subsequent higher resolution dataset generated by Sweere *et al.* (2020). The latter has been evaluated and those $\delta^{13}C$ values corresponding with bentonite beds have been removed as they do not reflect the global carbon cycle. The resultant cleaned $\delta^{13}C$ data spanning the MCE interval in the Iona-1 core is presented in Figure 2. The two $\delta^{13}C$ maxima

characterising the MCE are clearly defined, with MCE 1a occurring between 142.8 and 141.3 m, and MCE 1b between 139.9 and 139.5 m. A small positive shift in $\delta^{13}C$ values at 143.73 m prior to MCE 1a is interpreted to reflect the MCE initiation (Eldrett *et al.*, 2015). The higher resolution $\delta^{13}C$ data provided by Sweere *et al.* (2020) provides additional constraint for the MCE termination, which is selected at 139.50 m, slightly deeper than original lower resolution $\delta^{13}C$ dataset (*ca.* 139.27 m; Eldrett *et al.*, 2015).

The MCE profile characterised at Iona-1 is comparable to other records, such as Pueblo, USA and Folkestone, UK (see Figure 1). Both the MCE 1a and 1b are correlatable, with a similar shift/build-up phase marking the initiation (Figure 1). The assignment of this interval in Iona-1 to the MCE is further constrained by biostratigraphy, with the first common occurrence of the dinoflagellate cyst *Litosphaeridium siphoniphorum* at 144.21 m defining the top of the *Ovoidinium verrucosum* Interval Zone (Dodsworth and Eldrett, 2019). The *Ovoidinium verrucosum* Interval Zone corresponds with the MCE interval in the USGS Portland-1 core (Dodsworth and Eldrett, 2019). In addition, the first occurrence of the planktonic foraminifera *Rotalipora cushmani* at 133.68 m is just above the MCE in the Iona-1 core (Eldrett *et al.*, 2015) and occurs in a similar stratigraphic position in relation to the MCE interval in the Folkestone-Dover Chalk sections, UK (after Moghadam and Paul, 2000).

Furthermore, astronomical time series analyses have also been conducted on the Iona-1 core (Eldrett *et al.*, 2015; Ma *et al.*, 2019, 2020, 2022). These analyses indicate the onset of the MCE at 96.58 ± 0.12 Ma (143.73 m) and terminating at 96.36 ± 0.12 Ma (139.50 m). The MCE 1a excursion occurs between 142.8 m and 141.3 m with an astronomically tuned age of 96.53–96.46 Ma ± 0.12 Ma. This age assignment is consistent with the age of the Thatcher bentonite in the *Conlinceras tarrantense* zone and within first peak of the MCE at Pueblo, Colorado (Gale *et al.*, 2008; Figure 1), which yielded an $^{40}Ar/^{39}Ar$ age of 96.21 ± 0.16 (2σ analytical uncertainty) or ±0.36 (full uncertainty; Batenburg *et al.*, 2016). Further astronomic tuning of the Thatcher bentonite level by Batenburg *et al.* (2016) provided an additional constraint suggesting an age of either 96.09 ± 0.15 Ma (tuning 1) or 96.49 ± 0.15 Ma (tuning 2). Tuning option 2 is almost identical to Eldrett *et al.* (2015)

and Ma *et al.* (2020, 2022) and within the total uncertainty of the $^{40}Ar/^{39}Ar$ age of the Thatcher bentonite. This analysis indicates that the MCE-1a event is consistently identified between the Pueblo outcrop section and the Iona-1 core.

In the Iona-1 core, additional positive shifts in $\delta^{13}C$ values are recorded in the basal section of the lower Eagle Ford Fm. (147.23–150.8 m) and occur within the early Cenomanian and not considered part of the MCE. This interval was assigned to the mid-dixoni and lower Cenomanian $\delta^{13}C$ Events (Eldrett *et al.*, 2015; Minisini *et al.*, 2018). This early Cenomanian age assignment is further supported by the correlation of the Iona-1 core with outcrop sections along Highway 90, Texas (Minisini *et al.*, 2018). Zircons in bentonites from the outcrop sections were analysed using CA-TIMS U-Pb dating and yield the following ages (Minisini *et al.*, 2018): 96.97 ± 0.2 Ma (T8B; 5.1 m above Buda contact, outcrop DR-19); 97.4 ± 0.2 Ma (T9; 2.7 m above Buda contact, outcrop DR-19); 97.65 ± 0.12 Ma (T10; 0.4 m above Buda contact, outcrop DR-26) and 97.89 ± 0.25 Ma (T11; youngest grain analysed at 98.45 ± 0.11 Ma [weighted mean], 0 m above Buda contact, outcrop DR-19). The dates constrain the basal Eagle Ford Group age, with at least the basal five meters corresponding to the Early Cenomanian. The overlying dual positive peak $\delta^{13}C$ maxima in the Iona-1 core occurs approximately nine meters above the Eagle Ford–Buda Fm. contact and as supported by the available biostratigraphic constraints and astronomically tuned age models clearly corresponds with the MCE.

Materials and Analytical Method

The MCE is identified by carbon isotope ($\delta^{13}C$) records from both marine carbonate and organic carbon records by a characteristic dual positive carbon isotope excursion consisting of two $\delta^{13}C$ maxima (MCE a and MCE b, respectively; Mitchell *et al.*, 1996). In the Iona-1 core, of the Western Interior Seaway (WIS; Fig. 2) the interval is characterised by a dual positive $\delta^{13}C$ excursion and composed of marlstones and limestones of the Eagle Ford Group (Eldrett *et al.*, 2015) (Fig. 1). In brief, Os and Re concentration data were obtained from 0.4 g sample powders. These were digested using reverse aqua regia in Carius tubes. A mixed ^{99}Ru, ^{105}Pd, ^{185}Re, ^{190}Os, ^{191}Ir, and ^{194}Pt spike was added for concentration measurements via isotope dilution.

The Carius tubes were heated at 240 °C for 48 hours. Following digestion, the Carius tubes were removed, and the Os extracted from the solution using $CHCl_3$ followed by back-extraction into 9 N HBr (Cohen and Waters, 1996). The HBr solutions containing Os were dried down, and the residues were further purified by microdistillation with a CrO_3-H_2SO_4 solution and collected in 9 N HBr. The Os isotope compositions were determined using a ThermoFisher Triton, thermal ionisation mass spectrometer (TIMS) in negative mode, with a secondary electron multiplier using peak hopping mode at the University of Houston. The long-term average and precision of $^{187}Os/^{188}Os$ for the UMD Os standard using the SEM is 0.11380934 ± 0.00033913 (2 s.d.) with $N = 49$ and within error of the accepted value of 0.1138067 ± 0.000021 (Brandon *et al.*, 1999).

The residual solutions after Os removal, containing Re, were dried at 80 °C. The dried residues were dissolved in 6 N HCl and taken to dryness. This step was repeated twice to ensure full conversion to the chloride form. The sample solutions were then be passed through Eichrom AG 1-X8 100–200 mesh anion resin following a modified procedure from Day *et al.* (2016). The collected Re fractions were dried down, then converted to chloride form by redissolving in HCl. The Re fractions were then further purified using Eichrom AG 50-X8 100–200 mesh cation resin following the procedure of Puchtel and Humayun (2001). After purification, ^{185}Re and ^{187}Re were measured on an Agilent 8800 Triple Quadrupole ICP-MS at the University of Houston, in a NH_3 carrier gas and on the Element XR at the Williams Radiogenic Laboratory at Texas A&M University. This ensures minimisation of isotopic interferences while maximising signal intensities. Mass fractionation factors were determined by sample/standard bracketing using a standard of natural isotopic composition and then applying the obtained exponential mass fractionation factor to the sample measurements. Procedural blanks were 1.4 pg for Os and 41 pg for Re.

In addition to the samples reported in Table 1, a subset of samples were also measured as well as above and below the MCE to check for estimate the background Os_i leading up to and after the MCE, however, they were challenging to incorporate with the MCE interval samples because they are as it turns out not only

associated with other very small carbon isotope excursion (a phenomenon characteristic of the Mesozoic) below the MCE and or close to the unconformity below the MCE around 149 m, but the carbon resolution in this part core to make any meaningful interpretation too far outside the MCE interval. Additionally, a subset was measured for other platinum group elements and are presented below in Table S-1. The Ru, Pd, Pt, like the Re isotopes were measured in a NH_3 carrier gas, and Ir isotopes were measured in a He carrier gas. This is to ensure minimisation of isotopic interferences while maximising signal intensities. The HSE results did not show any spike that could be indicative of extraterrestrial inputs.

Supplementary Table

Table S-1 Platinum group element abundances of selected samples during the MCE interval in the Iona-1 core.

Depth	Age	Re (ppb)	Os (ppt)	$^{187}Os/^{188}Os$ measured	±2σ	$^{187}Re/^{188}Os$	±2σ	$^{187}Os/^{188}Os$ initial	±2σ	Ir (ppb)	Ru (ppb)	Pt (ppb)	Pd (ppb)
132.45	96.00	30	116	4.16	0.02	1907	8	1.109	0.04				
132.45	96.00	27	100	4.38	0.02	1998	6	1.179	0.03				
132.76	96.02	167	455	6.05	0.02	3141	10	1.017	0.04				
133.68	96.06	167	513	5.25	0.02	2611	9	1.070	0.03				
134.65	96.11	32	87	6.49	0.04	3241	12	1.290	0.06				
136.14	96.19	115	563	5.01	0.05	2555	20	0.91	0.02	0.028	0.116	3.649	2.365
137.31	96.25	27	142	4.86	0.04	2401	23	1.00	0.00	0.097	0.011	0.401	2.515
137.85	96.28	113	528	5.44	0.09	2775	31	0.99	0.04	0.016	0.043	0.634	3.528
139.27	96.36	18	102	4.06	0.04	2017	23	0.82	0.00	0.010	0.007	0.332	0.048
139.86	96.39	110	656	3.68	0.03	1878	14	0.66	0.01	0.287	0.150	3.362	4.687
140.39	96.42	100	562	4.36	0.01	2125	14	0.94	0.01	0.013	0.037	1.581	0.856
141.15	96.45	147	751	5.07	0.02	2471	16	1.10	0.01	0.356	0.064	0.795	54.797
141.77	96.48	15	76	5.21	0.07	2453	36	1.26	0.02	0.005	0.014	0.542	0.169
142.27	96.50	92	470	5.03	0.03	2447	17	1.09	0.00	0.025	0.080	1.216	0.327
143.37	96.56	127	753	4.05	0.01	1962	13	0.89	0.01	0.006	0.059	2.749	0.850
144.63	96.62	159	794	5.34	0.05	2675	22	1.03	0.02	0.079	0.062	2.047	−0.010
145.75	96.67	184	854	5.73	0.10	2975	166	0.93	0.17	0.038	0.049	1.305	−0.021
146.46	96.70	250	1038	6.28	0.08	3330	32	0.91	0.03	−0.010	−0.012	0.173	0.121
147.86	96.77	233	869	3.83	0.10	1918	29	0.730	0.15				
147.86	96.77	252	725	5.70	0.02	2892	11	1.034	0.04				
149.57	96.86	287	864	5.28	0.02	2678	31	0.953	0.07				
150.15	96.89	374	1237	4.51	0.01	2288	20	0.807	0.05				

Supplementary Figure

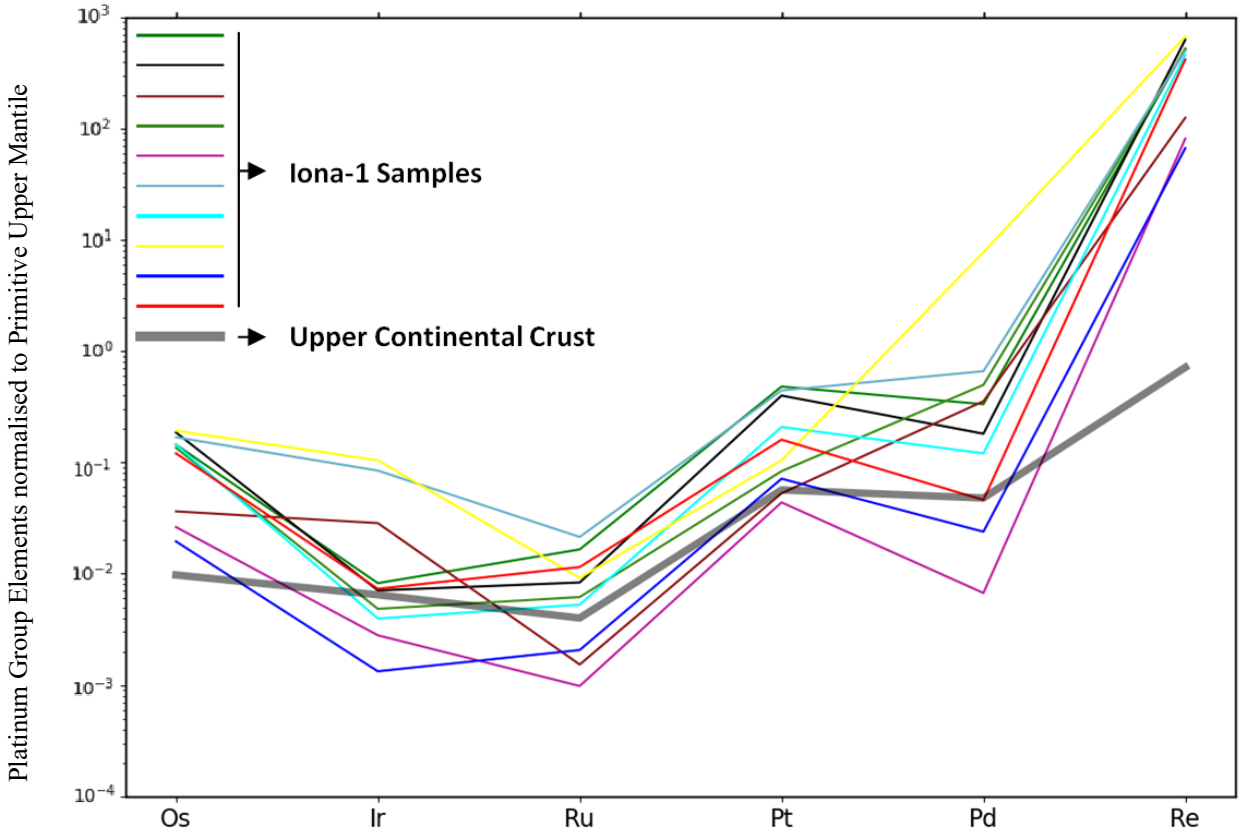

Figure S-1 HSE abundance normalised to primitive upper mantle (Becker *et al.*, 2006) of the samples from the MCE interval of the Iona-1 core compared to an average upper continental crustal value (Chen *et al.*, 2016).

Supplementary Information References

Andrieu, S., Brigaud, B., Rabourg, T., Noret, A. (2015) The Mid-Cenomanian Event in shallow marine environments: Influence on carbonate producers and depositional sequences (northern Aquitaine Basin, France). *Cretaceous Research* 56, 587–607. https://doi.org/10.1016/j.cretres.2015.06.018

Batenburg, S.J., De Vleeschouwer, D., Sprovieri, M., Hilgen, F.J., Gale, A.S., Singer, B.S., Koeberl, C., Coccioni, R., Claeys, P., Montanari, A. (2016) Orbital control on the timing of oceanic anoxia in the Late Cretaceous. *Climate of the Past* 12, 1995–2009. https://doi.org/10.5194/cp-12-1995-2016

Becker, H., Horan, M.F., Walker, R.J., Gao, S., Lorand, J.-P., Rudnick, R.L. (2006) Highly siderophile element composition of the Earth's primitive upper mantle: Constraints from new data on peridotite massifs and xenoliths. *Geochimica et Cosmochimica Acta* 70, 4528–4550. https://doi.org/10.1016/j.gca.2006.06.004

Brandon, A.D., Norman, M.D., Walker, R.J., Morgan, J.W. (1999) ^{186}Os-^{187}Os systematics of Hawaiian picrites. *Earth and Planetary Science Letters* 174, 25–42. https://doi.org/10.1016/S0012-821X(99)00251-4

Chen, K., Walker, R.J., Rudnick, R.L., Gao, S., Gasching, R.M., Puchtel, I.S., Tang, M., Hu Z.-C. (2016) Platinum-group element abundances and Re–Os isotopic systematics of the upper continental crust through time: Evidence from glacial diamictites. *Geochimica et Cosmochimica Acta* 191, 1–16. https://doi.org/10.1016/j.gca.2016.07.004

Coccioni, R., Galeotti, S. (2003) The mid-Cenomanian Event: prelude to OAE 2. *Palaeogeography, Palaeoclimatology, Palaeoecology* 190, 427–440. https://doi.org/10.1016/S0031-0182(02)00617-X

Cohen, A.S., Waters, F.G. (1996) Separation of osmium from geological materials by solvent extraction for analysis by thermal ionization mass spectrometry. *Analytica Chimica Acta* 332, 269–275. https://doi.org/10.1016/0003-2670(96)00226-7

Day, J.M.D., Waters, C.L., Schaefer, B.F., Walker, R.J., Turner, S. (2016) Use of Hydrofluoric Acid Desilicification in the Determination of Highly Siderophile Element Abundances and Re-Pt-Os Isotope Systematics in Mafic-Ultramafic Rocks. *Geostandards and Geoanalytical Research* 40, 49–65. https://doi.org/10.1111/j.1751-908X.2015.00367.x

Dodsworth, P., Eldrett, J.S. (2019) A dinoflagellate cyst zonation of the Cenomanian and Turonian (Upper Cretaceous) in the Western Interior, United States. *Palynology* 43, 701–723. https://doi.org/10.1080/01916122.2018.1477851

Eldrett, J.S., Ma, C., Bergman, S.C., Lutz, B., Gregory, F.J., Dodsworth, P., Phipps, M., Hardas, P., Minisini, D., Ozkan, A., Ramezani, J., Bowring, S.A., Kamo, S.L., Ferguson, K., Macaulay, C., Kelly, A.E. (2015) An astronomically calibrated stratigraphy of the Cenomanian, Turonian and earliest Coniacian from the Cretaceous Western Interior Seaway, USA: Implications for global chronostratigraphy. *Cretaceous Research* 56, 316–344. https://doi.org/10.1016/j.cretres.2015.04.010

Friedrich, O., Erbacher, J., Wilson, P.A., Moriya, K., Mutterlose, J. (2009) Paleoenvironmental changes across the Mid Cenomanian Event in the tropical Atlantic Ocean (Demerara Rise, ODP Leg 207) inferred from benthic foraminiferal assemblages. *Marine Micropaleontology* 71, 28–40. https://doi.org/10.1016/j.marmicro.2009.01.002

Gale, A.S., Hardenbol, J., Hathway, B., Kennedy, W.J., Young, J.R., Phansalkar, V. (2002) Global correlation of Cenomanian (Upper Cretaceous) sequences: Evidence for Milankovitch control on sea level. *Geology* 30, 291–294. https://doi.org/10.1130/0091-7613(2002)030<0291:GCOCUC>2.0.CO;2

Gale, A.S., Voigt, S., Sageman, B.B., Kennedy, W.J. (2008) Eustatic sea-level record for the Cenomanian (Late Cretaceous)—Extension to the Western Interior Basin, USA. *Geology* 36, 859–862. https://doi.org/10.1130/G24838A.1

Gambacorta, G., Jenkyns, H.C., Russo, F., Tsikos, H., Wilson, P.A., Faucher, G., Erba, E. (2015) Carbon- and oxygen-isotope records of mid-Cretaceous Tethyan pelagic sequences from the Umbria–Marche and Belluno Basins (Italy). *Newsletters on Stratigraphy*, 48, 299–323. https://doi.org/10.1127/nos/2015/0066

Gertsch, B., Adatte, T., Keller, G., Tantawy, A.A.A.M., Berner, Z., Mort, H.P., Fleitmann, D. (2010) Middle and late Cenomanian oceanic anoxic events in shallow and deeper shelf environments of western Morocco. *Sedimentology* 57, 1430–1462. https://doi.org/10.1111/j.1365-3091.2010.01151.x

Jarvis, I., Murphy, A.M., Gale, A.S. (2001) Geochemistry of pelagic and hemipelagic carbonates: criteria for identifying systems tracts and sea-level change. *Journal of the Geological Society* 158, 685–696. https://doi.org/10.1144/jgs.158.4.685

Jarvis, I., Gale, A.S., Jenkyns, H.C., Pearce, M.A. (2006) Secular variation in Late Cretaceous carbon isotopes: a new $\delta^{13}C$ carbonate reference curve for the Cenomanian–Campanian (99.6–70.6 Ma). *Geological Magazine* 143, 561–608. https://doi.org/10.1017/S0016756806002421

Joo, Y.J., Sageman, B.B. (2014) Cenomanian To Campanian Carbon Isotope Chemostratigraphy from the Western Interior Basin, U.S.A. *Journal of Sedimentary Research* 84, 529–542. https://doi.org/10.2110/jsr.2014.38

Li, X., Jenkyns, H.C., Wang, C., Hu, X., Chen, X., Wei, Y., Huang, Y., Cui, J. (2006) Upper Cretaceous carbon- and oxygen-isotope stratigraphy of hemipelagic carbonate facies from southern Tibet, China. *Journal of the Geological Society* 163, 375–382. https://doi.org/10.1144/0016-764905-046

Ma, C., Meyers, S.R., Sageman, B.B. (2019) Testing Late Cretaceous astronomical solutions in a 15 million year astrochronologic record from North America. *Earth and Planetary Science Letters* 513, 1–11. https://doi.org/10.1016/j.epsl.2019.01.053

Ma, C., Meyers, S.R., Hinnov, L.A., Eldrett, J.S., Bergman, S.C., Minisini, D. (2020) A method to decipher the time distribution in astronomically forced sedimentary couplets. *Marine and Petroleum Geology* 118, 104399. https://doi.org/10.1016/j.marpetgeo.2020.104399

Ma, C., Hinnov, L.A., Eldrett, J.S., Meyers, S.R., Bergman, S.C., Minisini, D., Lutz, B. (2022) Centennial to millennial variability of greenhouse climate across the mid-Cenomanian event. *Geology* 50, 227–231. https://doi.org/10.1130/G48734.1

Minisini, D., Eldrett, J., Bergman, S.C., Forkner, R. (2018) Chronostratigraphic framework and depositional environments in the organic-rich, mudstone-dominated Eagle Ford Group, Texas, USA. *Sedimentology* 65, 1520–1557. https://doi.org/10.1111/sed.12437

Mitchell, S.F. (1996) Foraminiferal assemblages from the late Lower and Middle Cenomanian of Speeton (North Yorkshire, UK): relationships with sea-level fluctuations and watermass distribution. *Journal of Micropalaeontology* 15, 37–54. https://doi.org/10.1144/jm.15.1.37

Mitchell, S.F., Carr, I.T. (1998) Foraminiferal response to mid-Cenomanian (Upper Cretaceous) palaeoceanographic events in the Anglo-Paris Basin (Northwest Europe). *Palaeogeography, Palaeoclimatology, Palaeoecology* 137, 103–125. https://doi.org/10.1016/S0031-0182(97)00087-4

Mitchell, S.F., Paul, C.R.C., Gale, A.S. (1996) Carbon isotopes and sequence stratigraphy. In: Howell, J.A., Aitken, J.F. (Eds.) *High Resolution Sequence Stratigraphy: Innovations and Applications*. Geological Society of London, Special Publication 104, 11–24. https://doi.org/10.1144/GSL.SP.1996.104.01.02

Moghadam, H.V., Paul, C.R.C. (2000) Micropalaeontology of the Cenomanian at Chinnor, Oxfordshire, and comparison with the Dover-Folkestone succession. *Proceedings of the Geologists' Association* 111, 17–39. https://doi.org/10.1016/S0016-7878(00)80034-6

Paul, C.R.C., Mitchell, S.F., Marshall, J.D., Leary, P.N., Gale, A.S., Duane, A.M., Ditchfield, P.W. (1994) Paleoceanographic events in the Middle Cenomanian of Northwest Europe. *Cretaceous Research* 15, 707–738. https://doi.org/10.1006/cres.1994.1039

Puchtel, I.S., Humayun**,** M. (2001) Platinum group element fractionation in a komatiitic basalt lava lake. *Geochimica et Cosmochimica Acta* 65, 2979–2993. https://doi.org/10.1016/S0016-7037(01)00642-1

Stoll, H.M., Schrag, D.P. (2000) High-resolution stable isotope records from the Upper Cretaceous rocks of Italy and Spain: Glacial episodes in a greenhouse planet? *Geological Society of America Bulletin* 112, 308–319. https://doi.org/10.1130/0016-7606(2000)112<308:HSIRFT>2.0.CO;2

Sweere, T.C., Dickson, A.J., Jenkyns, H.C., Porcelli, D., Ruhl, M., Murphy, M.J., Idiz, E., van den Boorn, S.H.J.M., Eldrett, J.S., Henderson, G.M. (2020) Controls on the Cd-isotope composition of Upper Cretaceous (Cenomanian–Turonian) organic-rich mudrocks from south Texas (Eagle Ford Group). *Geochimica et Cosmochimica Acta* 287, 251–262. https://doi.org/10.1016/j.gca.2020.02.019

Wilmsen, M. (2007) Integrated stratigraphy of the upper Lower–lower Middle Cenomanian of northern Germany and southern England. *Acta Geologica Polonica* 57, 263–279. https://geojournals.pgi.gov.pl/agp/article/view/9806